Results in Physics 38 (2022) 105661

Contents lists available at ScienceDirect

Results in Physics

journal homepage: www.elsevier.com/locate/rinp

Inelastic soliton wave solutions with different geometrical structures to fractional order nonlinear evolution equations

M. Adel [a], Dumitru Baleanu [b,c,d,*], Umme Sadiya [e], Mohammad Asif Arefin [e], M. Hafiz Uddin [e], Mahjoub A. Elamin [f], M.S. Osman [g,**]

[a] Department of Mathematics, Faculty of Science, Islamic University of Madinah, Medina, Saudi Arabia
[b] Department of Mathematics, Faculty of Arts and Sciences, Cankaya University, Ogretmenler Cad. 1406530, Ankara, Turkey
[c] Institute of Space Sciences, Magurele, Bucharest, Romania
[d] Department of Medical Research, China Medical University Hospita, China Medical University, Taichung, Taiwan
[e] Department of Mathematics, Jashore University of Science and Technology, Jashore 7408, Bangladesh
[f] Department of Mathematics, University College of Umluj, Tabuk University, Saudi Arabia
[g] Department of Mathematics, Faculty of Science, Cairo University, Giza 12613, Egypt

ARTICLE INFO

Keywords:
The TF-BF equation
The STF-RLW equation
The CFD
The ET-F technique

ABSTRACT

The general time fractional Burger- Fisher (TF-BF) and the space–time regularized long-wave (STF-RLW) equations are considered as examples of gravitational water waves in cold plasma as well as so many areas. The above equations are used in nonlinear science and engineering to study long waves in seas and harbors that travel in just one direction. First, the two equations are transformed to ODEs by applying a fractional complex transform along with characteristics of confirmable fractional derivative (CFD). Then, the extended tanh-function (ET-F) approach is investigated to find a variety of analytical solutions with different geometrical wave structures the mentioned models. The results are in the form of kink, one-, two-, multiple-solitons solutions, and other types sketched in 2D, 3D, and contour patterns.

Introduction

Fractional derivatives, including the issue of sense of extension, made their debut in 1695. Fractional calculus offers realistic discussions of real-world phenomena better than classical one [1–3]. Throughout the twentieth centenary, several pioneers conducted a vast quantity of experiments on fractional calculus. A lot of beginners such as Caputo, M., Fabrizio, M. [4], Bin, Z. [5], Cermak, Jan, and Tomas Kisela [6], Ahmed, E., A. S. Elgazzar [7], and others conducted a considerable amount of research on fractional calculus. Problems have recently been solved using nonlinear fractional differential equations (NLFDEs) in many different fields of applied sciences. Magnetism, acoustic wave transmission in rigid porous materials, cardiac tissue electrode interface, the theory of viscoelasticity, aerodynamics, ultrasonic wave wave propagation in human malignant bone, RLC electric circuit, heat transfer, and other applications can all benefit from NLFDEs. As a result, numerous processes for determining the exact resolution of NLFDEs have been established. Among these process: Adomian's decomposition algorithm [8–10], differential transformation method [11,12], variational iteration technique [13–15], homotopy analysis scheme [16,17], the finite element method [18], the (G'/G) expansion method [19–20], the sine-Gordon expansion method [21], the generalized unified method [22], the exp-function method [23], An efficient variable stepsize rational method [24], the reproducing kernel algorithm [25], the modified kudrayshov approach [26], the fractional sub-equation method [27–30], the first integral method [31], the modified reproducing kernel discretization technique [32], the double $(G'/G,\ 1/G)$ -expansion method [33–35], and several others [36–44].

Burgers-Fisher equation is a nonlinear equation combining reaction, convection, and diffusion mechanisms. Johannes Martinus Burgers (1895–1981) [45–47] established the mathematical framework of Burgers' equation. lately in the discipline of fractional calculus, tremendous

* Corresponding authors at: Department of Mathematics, Faculty of Arts and Sciences, Cankaya University, Ogretmenler Cad. 1406530, Ankara, Turkey (D. Baleanu).
** Corresponding authors at: Department of Mathematics, Faculty of Science, Cairo University, Giza 12613, Egypt (M.S. Osman).
E-mail addresses: m.adel@iu.edu.sa (M. Adel), dumitru@cankaya.edu.tr (D. Baleanu), asif.math@just.edu.bd (M. Asif Arefin), mh.uddin@just.edu.bd (M. Hafiz Uddin), Malshaygi@ut.edu.sa (M.A. Elamin), mofatzi@cu.edu.eg (M.S. Osman).

https://doi.org/10.1016/j.rinp.2022.105661
Received 29 April 2022; Received in revised form 17 May 2022; Accepted 25 May 2022
Available online 27 May 2022

progress has been accomplished. The origin and distinctiveness of solutions to a class of stochastic differential equations generalized Burgers' equations powered by multi-parameter fractional noises are demonstrated in [48]. In the context of nonlinear wave propagation in porous media, Garra [49] defined an application of the time-fractional Burgers' equation (TF-BE). The variational iteration method (VIM) [50] and the homotopy perturbation method (HPM) [51] be accustomed to solving the Burgers' equation with time and space time fractional derivatives, respectively. Chemical kinetics [52], nonlinear heat conduction [53], branching Brownian motion [54], epidemics, and bacteria [55] are some of the other applications of this model. The TF-BF equation is useful in a variety of situations such as financial mathematics, gas dynamics, and traffic flow, applied number theory, and elasticity. The general TF-BF equation can be formed as [56],

$$\frac{\partial^\alpha u}{\partial t^\alpha}+\rho u\frac{\partial u}{\partial x}-\frac{\partial^2 u}{\partial x^2}=\beta u(1-u), \tag{1.1}$$

where ρ and β are real parameters and $0<\alpha\le 1$. This equation is also used in fluid dynamics, heat conduction, elasticity, and capillary-gravity waves.

In mathematical sciences and technologies, the regularized long wave (RLW) equation is used to interpret the one-way track of long waves in seas and harbors. Many physical occurrences, such as ion sound waves in plasma and moving waves with space-charge, are studied using the RLW equation. Peregrine was the first to implement this approach in [57], and it has since been successfully used to solve a variety of ill-posed problems, parabolic equation [58], inverse time-dependent heat source problem [59], determining the heat source [60], regularization of exponentially ill-posed problems [61], the basis of a reproducing kernel space [62]. The STF-RLW equation has the following structure [63],

$$D_t^\alpha u(x,t)+D_x^\alpha u(x,t)+\varepsilon D_x^\alpha u^2(x,t)-\mu D_{xxt}^{3\alpha}u(x,t)=0. \tag{1.2}$$

Here, D_t^α is the fractional derivative of order $0<\alpha\le 1$ and ε,μ are real parameters. Eq. (1.2) arises in different physical fields including ion sound waves in plasma. For $\alpha=1$, this equation refers to weakly nonlinear ion acoustic and space-charge waves.

The next portion of the article is organized as follows: the confirmable fractional derivative is discussed in segment 2. The proposed adapted extended tanh-function (ET-F) method is used in segment 3. Applications of our mentioned method are investigated in segment 4. Some graphical plots and discussion are presented in segment 5. The conclusions are presented in the final segment.

Definitions and prefaces

Let $f:\mathbb{R}^{\ge 0}\to\mathbb{R}$. The α-order "conformable derivative'' for f can be stated as [64]:

$$M_\alpha(f)(t)=\lim_{\varepsilon\to 0}\frac{f(t+\varepsilon t^{1-\alpha})-f(t)}{\varepsilon}. \tag{2.1}$$

for all positive $t, 0<\alpha\le 1$.

If f be α-differentiable in some $(0,a), a>0$ and $\lim_{t\to 0^+}f^{(\alpha)}(t)$ exists, then $f^{(\alpha)}(0)=\lim_{t\to 0^+}f^{(\alpha)}(t)$.

Proposition 1. Assume $\alpha\in(0,1]$ and suppose f,g be α-differentiable at a point $t>0$. Hence

- $M_\alpha(xf+yg)=xM_\alpha(f)+yM_\alpha(g)$, for all $x,y\in\mathbb{R}$.
- $M_\alpha(t^z)=zt^{p-\alpha}$, for all $z\in\mathbb{R}$.
- $M_\alpha(u)=0$, for all constant function $f(t)=u$.
- $M_\alpha(fg)=fM_\alpha(g)+gM_\alpha(f)$.
- $M_\alpha\left(\frac{f}{g}\right)=\frac{gM_\alpha(f)-fM_\alpha(g)}{g^2}$.
- In addition, if f is differentiable, then $MT_\alpha(f)(t)=t^{1-\alpha\frac{df}{dt}}$.

Khalilet al. [64] discusses some additional properties related to the CFD, such as the Laplace transform, Tailor series expansion, chain rule, Gronwall's inequality, and integration methods.

Proposition 2. Assume f is an α-differentiable function in conformable differentiable sense and suppose that g is differentiable and lies in the range of f, then

$$M_\alpha(f^\circ g)(t)=t^{1-\alpha}g'(t)f_g(t) \tag{2.2}$$

Fundamental facts and the implementation of the method

The ET-F method [65] for obtaining exact solutions for the NLFDEs is described here. To start with, we apprehend the following NLFDE R associated with a function $U=U(x,t)$:

$$R\left(u,D_t^\alpha u,D_x^\beta u,D_t^\alpha D_t^\alpha u,D_t^\alpha D_x^\beta u,D_x^\beta D_x^\beta,\cdots\cdots\right)=0,0<\alpha\le 1,0<\beta\le 1 \tag{3.1}$$

u is an arbitrary function in its arguments. Consider the transformation of waves:

$$\xi=k\frac{x^\beta}{\beta}+c\frac{t^\alpha}{\alpha},u(x,t)=u(\xi) \tag{3.2}$$

here c and k are nonzero constants.

Applying Eq. (3.2) on (3.1), we get the following ODE:

$$R(u,u',u'',u''',\cdots\cdots)=0 \tag{3.3}$$

where the superscripts indicate the ordinary derivative of u.

Phase 1: The general solution of Eq. (3.3) is assumed to be in the following type:

$$u(\xi)=\sum_{i=0}^n a_iY^i+\sum_{i=1}^n b_iY^{-i} \tag{3.4}$$

$$Y=\tanh(\mu\xi) \tag{3.5}$$

where μ is an arbitrary value.

Phase 2: The positive constant η can be identified by applying the homogeneous balance condition between the maximum order and the highest degree of nonlinear terms in Eq. (3.3).

Phase 3: Embedding (3.4) and (3.5) into Eq. (3.3) leads to a polynomial in Y. Setting its coefficients equal zero yields a system of algebraic equations in $a_i's$ and $b_i's$ which can be solved using any package of symbolic computation software.

Phase 4: Different closed form solutions for Eq. (3.3) can be established by inserting the obtained in Phase 3 in Eq. (3.4) in the presence of Eq. (3.5).

Analysis of the solutions

Using the ET-F process, we develop abundant wave solutions to the TF-BF and STF-RLW equations.

The general TF-BF equation

The above-mentioned method is used in this part to investigate more detailed about exact analytic wave solutions for the TF-BF equation. The recommended equation recounts the physical methods of one-way stretch of dimly nonlinear phonetic waves through a gas-filled pipe. The memory effect of the wall friction through the boundary layer causes the fractional derivative. Waves in bubbly liquids and shallow-water waves are two examples of structures of the same form. For the Eq. (1.1), we advise the following transformation.

$$\delta = kx + \eta\frac{t^\alpha}{\alpha}, u(x,t) = u(\delta) \tag{4.1}$$

where η be the velocity of traveling wave. Applying Eq. (4.2) into Eq. (1.1) diminishes to the next ODE:

$$\eta u' + kpuu' - k^2u'' - \beta u + \beta u^2 = 0 \tag{4.2}$$

The homogeneous equilibrium transforms Eq. (3.4) into:

$$u(\delta) = a_0 + a_1 Y + a_2 Y^2 + b_1 Y^{-1} + b_2 Y^{-2} \tag{4.3}$$

Substituting (4.3) into (4.2) in the presence of (3.5), in Y, the left side transforms into a polynomial that gives a system of algebraic equations when setting its coefficients equal zero. The following results are obtained by using computer algebra, such as Maple, to solve this overdetermined series of equations:

Cluster 1:

$$\eta = \frac{1}{2}\frac{\beta}{\mu}, k = 0, a_0 = \frac{1}{2}, a_1 = \frac{1}{2}, a_2 = 0, \text{and } b_1 = 0, b_2 = 0$$

In terms of tanh functions, the values in cluster 1 yields an explicit solution in the following form:

$$u_1(x,t) = \frac{1}{2} + \frac{1}{2}\tanh(\sqrt{t}). \tag{4.4}$$

Cluster 2:

$$\eta = \frac{1}{4}\frac{\beta}{\mu}, k = 0, a_0 = \frac{1}{2}, a_1 = \frac{1}{4}, a_2 = 0 \text{and } b_1 = \frac{1}{4}, b_2 = 0$$

Cluster 2 gives another explicit solution as:

$$u_2(x,t) = \frac{1}{2} + \frac{1}{4}\tanh\left(\frac{\sqrt{t}}{2}\right) + \frac{1}{4}\coth\left(\frac{\sqrt{t}}{2}\right). \tag{4.5}$$

Cluster 3:

$\eta = -\frac{1}{8}\frac{4\beta^2+\rho^2}{\mu}$, $k = \frac{1}{4}\frac{\rho}{\mu}$, $a_0 = \frac{1}{2}, a_1 = 0, a_2 = 0$ and $b_1 = -\frac{1}{2}, b_2 = 0$.

In terms of sech function the values of the parameters presented in cluster 3 formulate an explicit solution:

$$u_3(x,t) = \frac{1}{2} - \frac{1}{2}\sqrt{1 - \operatorname{sech}(\frac{x}{4} - \frac{5\sqrt{t}}{4})^2}. \tag{4.6}$$

Cluster 4:

$\eta = \frac{1}{8}\frac{4\beta^2+\rho^2}{\mu}$, $k = -\frac{1}{4}\frac{\rho}{\mu}$, $a_0 = \frac{1}{2}, a_1 = 0, a_2 = 0$ and $b_1 = \frac{1}{2}, b_2 = 0$.

Cluster 4 presents the following solution:

$$u_4(x,t) = \frac{1}{2} - \frac{1}{2}\sqrt{1 - \operatorname{csch}\left(-\frac{x}{4} + \frac{5\sqrt{t}}{4}\right)^2}. \tag{4.7}$$

Cluster 5:

$\eta = \frac{1}{8}\frac{4\beta^2+\rho^2}{\mu}$, $k = \frac{1}{4}\frac{\rho}{\mu}$, $a_0 = \frac{1}{2}, a_1 = -\frac{1}{2}, a_2 = 0$ and $b_1 = 0, b_2 = 0$.

The norm of the parameters submitted in cluster 5 which shows an explicit solution in terms of coth function:

$$u_5(x,t) = \frac{1}{2} - \frac{1}{2}\coth\left(\frac{x}{4} - \frac{5\sqrt{t}}{4}\right). \tag{4.8}$$

Cluster 6:

$\eta = \frac{1}{8}\frac{4\beta^2+\rho^2}{\mu}$, $k = -\frac{1}{4}\frac{\rho}{\mu}$, $a_0 = \frac{1}{2}, a_1 = \frac{1}{2}, a_2 = 0$ and $b_1 = 0, b_2 = 0$.

These principles of the parameters presented in cluster 6 originate an explicit solution in terms of csch function:

$$u_6(x,t) = \frac{1}{2} - \frac{1}{2}\sqrt{1 - \operatorname{csch}\left(\frac{x}{4} - \frac{5\sqrt{t}}{4}\right)^2}. \tag{4.9}$$

Cluster 7:

$\eta = -\frac{1}{16}\frac{4\beta^2+\rho^2}{\mu}$, $k = \frac{1}{8}\frac{\rho}{\mu}$, , $a_0 = \frac{1}{2}, a_1 = \frac{1}{4}, a_2 = 0$ and.$b_1 = -\frac{1}{4}, b_2 = 0$

Cluster 7 gives:

$$u_8(x,t) = \frac{1}{2} - \frac{1}{4}\tanh\left(\frac{x}{8} - \frac{5\sqrt{t}}{8}\right) - \frac{1}{4}\coth\left(\frac{x}{8} - \frac{5\sqrt{t}}{8}\right). \tag{4.10}$$

Cluster 8:

$\eta = \frac{1}{16}\frac{4\beta^2+\rho^2}{\mu}$, $k = -\frac{1}{8}\frac{\rho}{\mu}$, $a_0 = \frac{1}{2}, a_1 = \frac{1}{4}, a_2 = 0$ and.$b_1 = \frac{1}{4}, b_2 = 0$

Cluster 8 is gained from those values of the parameters which create an explicit solution in terms of tanh and coth function.

$$u_8(x,t) = \frac{1}{2} + \frac{1}{4}\tanh\left(-\frac{x}{8} + \frac{5\sqrt{t}}{8}\right) + \frac{1}{4}\coth\left(-\frac{x}{8} + \frac{5\sqrt{t}}{8}\right). \tag{4.11}$$

Cluster 9:

$\eta = -\frac{1}{2}\frac{\beta}{\mu}$, $k = 0$, $a_0 = \frac{1}{2}, a_1 = \frac{1}{4}, a_2 = 0$ and.$b_1 = \frac{1}{4}, b_2 = 0$

In conditions of the tanh equation, Cluster 9 forms an explicit solution:

$$u_9(x,t) = \frac{1}{2} - \frac{1}{2}\tanh(\sqrt{-t}). \tag{4.12}$$

Cluster 10:

$\eta = -\frac{1}{4}\frac{\beta}{\mu}$, $k = 0$, $a_0 = \frac{1}{2}, a_1 = -\frac{1}{4}, a_2 = 0$ and.$b_1 = -\frac{1}{4}, b_2 = 0$

The principles of the parameters to be had in cluster 10 make an explicit solution in expressions of tanh and coth functions.

$$u_{10}(x,t) = \frac{1}{2} - \frac{1}{4}\tanh\left(-\frac{\sqrt{t}}{2}\right) + \frac{1}{4}\coth\left(-\frac{\sqrt{t}}{2}\right). \tag{4.13}$$

Cluster 11:

$\eta = \frac{1}{2}\frac{\beta}{\mu}$, $k = 0$, $a_0 = \frac{1}{2}, a_1 = \frac{1}{2}, a_2 = 0$ and.$b_1 = \frac{1}{2}, b_2 = 0$

The values of the parameters presented in cluster 11 formulate an explicit solution in terms of tanh function.

$$u_{11}(x,t) = \frac{1}{2} + \frac{1}{2\tanh(\sqrt{-t})}. \tag{4.14}$$

Cluster 12:

$\eta = -\frac{1}{2}\frac{\beta}{\mu}$, $k = 0$, $a_0 = \frac{1}{2}, a_1 = \frac{1}{2}, a_2 = 0$ and.$b_1 = -\frac{1}{2}, b_2 = 0$

Cluster 12 which is obtained from the given values of the parameters and gives:

$$u_{12}(x,t) = \frac{1}{2} - \frac{1}{2\tanh(\sqrt{-t})}. \tag{4.15}$$

The above results were obtained using the ET-F, which are novel and more general. These results have never been published before, as far as we know. The relativistic electron and the physical procedure of one-way stretch of weakly non-linear acoustic waves through a gas-filled pipe can both be defined using these solutions.

The STF-RLW equation

In this part, we look for more rigorous exact analytic wave solutions for the STF-RLW equation. For Eq. (1.2), we introduce the next transformation:

$$\xi = k\frac{x^\alpha}{\alpha} - c\frac{t^\alpha}{\alpha}, u(x,t) = u(\xi) \tag{4.16}$$

where c is the traveling wave velocity. When Eq. (4.16) is applied to Eq. (1.2), the next integral ODE emerges:

$$(k-c)u' + \varepsilon kuu' - \mu ck^2u'' = 0 \tag{4.17}$$

Integrating Eq. (4.17) with zero constant we obtain.

$$-cu + \frac{kpu^2}{2} - k^2vu' = 0. \tag{4.18}$$

Eq. (3.4) is reduced to the form by the homogeneous balance:

$$u(\xi) = a_0 + a_1 Y + a_2 Y^2 + b_1 Y^{-1} + b_2 Y^{-2} \tag{4.19}$$

Substituting (4.19) into (4.18) along with (3.5) and repeating the same steps in the previous section, we get a series of algebraic equations (for simplicity, we omit them to display) for a_0, a_1,a_2b_1, b_2, k and η. The following results are obtained by solving this over determined series of equations:

Cluster 1:

$c = \frac{k}{16\beta k^2\mu^2+1}$, $k = k$, $a_0 = -\frac{4\beta k^2\mu^2}{\varepsilon(16\beta k^2\mu^2+1)}$, $a_1 = 0, a_2 = -\frac{6\beta k^2\mu^2}{\varepsilon(16\beta k^2\mu^2+1)}$, and $b_1 = 0, b_2 = -\frac{4\beta k^2\mu^2}{\varepsilon\left(16\beta k^2\mu^2+1\right)}$.

Cluster 1 which is obtained from the given values of the parameters and gives an explicit resolution:

$$u_{13}(x,t) = -\frac{4}{17} - \frac{6}{17}\tanh^2\left(2\sqrt{x} - \frac{2\sqrt{t}}{17}\right) - \frac{6}{17}\coth^2\left(2\sqrt{x} - \frac{2\sqrt{t}}{17}\right). \quad (4.20)$$

The hyperbolic formula, as well as space and time coordinates, can be used to reconstruct it.

$$u_{14}(x,t) = -\frac{4}{17} - \frac{6}{17} + \frac{6}{17}\mathrm{sech}^2\left(2\sqrt{x} - \frac{2\sqrt{t}}{17}\right) - \frac{6}{17} - \frac{6}{17}\mathrm{csch}^2\left(2\sqrt{x} - \frac{2\sqrt{t}}{17}\right). \quad (4.21)$$

Cluster 2:

$c = \frac{k}{4\beta k^2\mu^2+1}$, $k = k$, $a_0 = \frac{2\beta k^2\mu^2}{\varepsilon(4\beta k^2\mu^2+1)}$, $a_1 = 0, a_2 = -\frac{6\beta k^2\mu^2}{\varepsilon(16\beta k^2\mu^2+1)}$ and $b_1 = 0, b_2 = 0$.

In terms of coth function, the values of the parameters given in cluster 2 form an explicit solution:

$$u_{15}(x,t) = \frac{2}{5} - \frac{6}{5}\tanh^2\left(2\sqrt{x} - \frac{2\sqrt{t}}{5}\right). \quad (4.22)$$

The hyperbolic formula and space, time coordinates can be used to reconstruct it.

$$u_{16}(x,t) = \frac{2}{5} - \frac{6}{5} + \frac{6}{5}\mathrm{sech}^2\left(2\sqrt{x} - \frac{2\sqrt{t}}{5}\right). \quad (4.23)$$

Cluster 3:

$c = -\frac{k}{4\beta k^2\mu^2-1}$, $k = k$, $a_0 = -\frac{6\beta k^2\mu^2}{\varepsilon(4\beta k^2\mu^2-1)}$, $a_1 = 0, a_2 = \frac{6\beta k^2\mu^2}{\varepsilon(4\beta k^2\mu^2-1)}$ and $b_1 = 0, b_2 = 0$.

The values of the parameters presented in cluster 3 formulate an explicit solution in terms of tanh function:

$$u_{17}(x,t) = -2 + 2\tanh^2\left(2\sqrt{x} + \frac{2\sqrt{t}}{3}\right). \quad (4.24)$$

The hyperbolic formula and space, time coordinates can then be used to reconstruct it.

$$u_{18}(x,t) = -2 + 2\left(1 - \mathrm{sech}^2\right)\left(2\sqrt{x} + \frac{2\sqrt{t}}{3}\right). \quad (4.25)$$

Cluster 4:

$c = \frac{k}{4\beta k^2\mu^2+1}$, $k = k$,$a_0 = \frac{1}{2}$, $a_1 = \frac{2\beta k^2\mu^2}{\varepsilon(4\beta k^2\mu^2+1)}$, $a_2 = 0$ and $b_1 = 0$, $b_2 = -\frac{6\beta k^2\mu^2}{\varepsilon(16\beta k^2\mu^2+1)}$.

In terms of coth functions, the values of the parameters given in cluster 4 form an explicit solution:

$$u_{19}(x,t) = \frac{2}{5} - \frac{6}{5}\coth^2\left(2\sqrt{x} - \frac{2\sqrt{t}}{5}\right). \quad (4.26)$$

The hyperbolic formula and space, time coordinates can be used to reconstruct it.

$$u_{20}(x,t) = \frac{2}{5} - \frac{6}{5}\left(1 - \mathrm{csch}^2\right)\left(2\sqrt{x} - \frac{2\sqrt{t}}{5}\right). \quad (4.27)$$

Cluster 5:

$c = \frac{k}{4\beta k^2\mu^2+1}$, kk, $a_0 = -\frac{6\beta k^2\mu^2}{\varepsilon(4\beta k^2\mu^2-1)}$, $a_1 = \frac{1}{2}$, $a_2 = 0$ and $b_1 = 0$, $b_2 = \frac{6\beta k^2\mu^2}{\varepsilon(4\beta k^2\mu^2-1)}$.

Principles of the parameters offered in cluster 5 originate an explicit solution in expressions of coth functions:

$$u_{21}(x,t) = -2 + 2\coth^2\left(2\sqrt{x} + \frac{2\sqrt{t}}{3}\right). \quad (4.28)$$

Which can be renovated by dint of the hyperbolic formula and space, time coordinates.

$$u_{22}(x,t) = -2 + 2\left(1 - csch^2\right)\left(2\sqrt{x} + \frac{2\sqrt{t}}{3}\right). \quad (4.29)$$

Cluster 6:

$c = -\frac{k}{16\beta k^2\mu^2-1}$, $k = k$, $a_0 = -\frac{12\beta k^2\mu^2}{\varepsilon(16\beta k^2\mu^2-1)}$, $a_1 = 0, a_2 = \frac{6\beta k^2\mu^2}{\varepsilon(16\beta k^2\mu^2-1)}$, and $b_1 = 0, b_2 = \frac{6\beta k^2\mu^2}{\varepsilon(16\beta k^2\mu^2-1)}$.

Cluster 6 is gained from those values of the parameters which

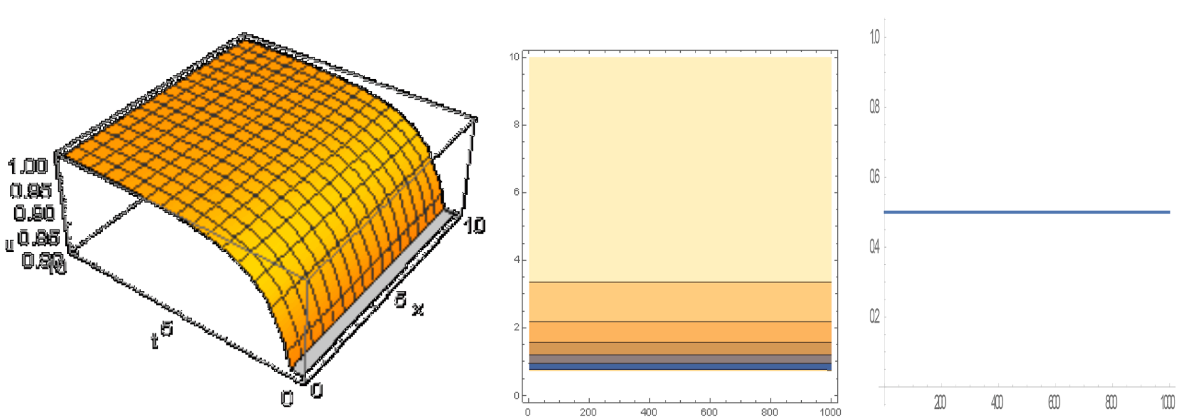

(a) 3D- diagram (b) Contour plot (c) 2D- diagram

Fig. 1. The kink type wave solution $u_1(x,t)$ within the intervals $0 < x < 10$ and $0 < t < 10$.

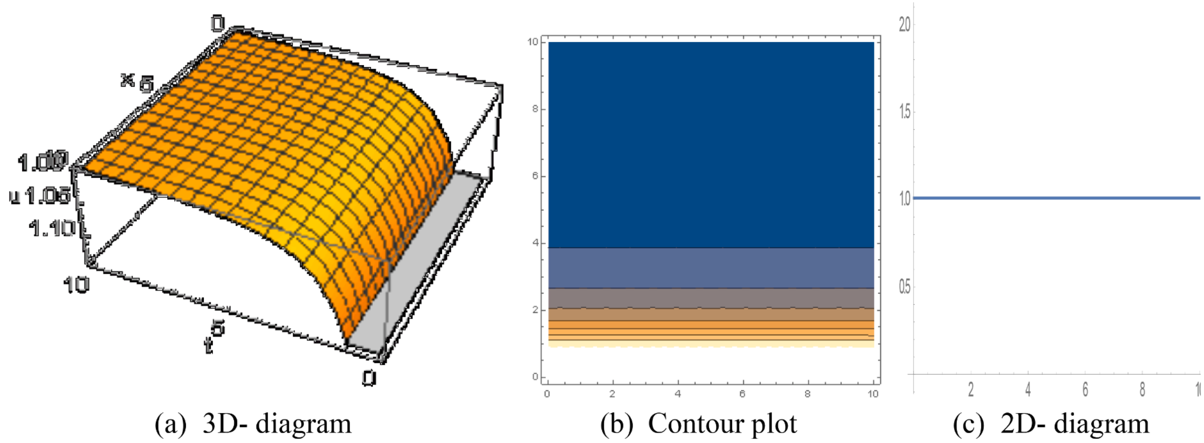

Fig. 2. The kink type wave solution $u_2(x,t)$ within the intervals $0 < x < 10$ and $0 < t < 10$.

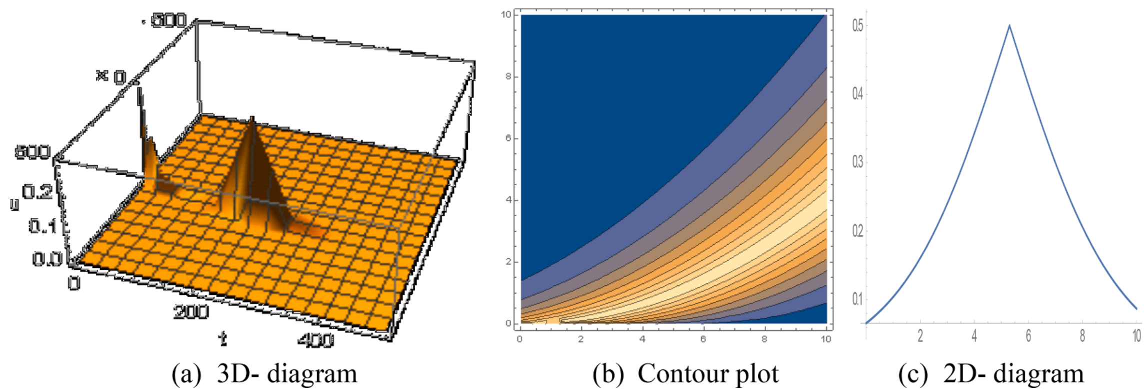

Fig. 3. The bell shape wave solution $u_3(x,t)$ within the intervals $0 < x < 10$ and $0 < t < 10$.

construct an explicit result in terms of tanh as well as coth functions:

$$u_{23}(x,t) = -\frac{12}{15}+\frac{6}{15}\tanh^2\left(2\sqrt{x}+\frac{2\sqrt{t}}{15}\right)+\frac{6}{15}\coth^2\left(2\sqrt{x}+\frac{2\sqrt{t}}{15}\right). \tag{4.30}$$

The hyperbolic formula and space, time coordinates can be used to rebuild it.

$$u_{24}(x,t) = -\frac{12}{15}+\frac{6}{15}-\frac{6}{15}\operatorname{sech}^2\left(2\sqrt{x}+\frac{2\sqrt{t}}{15}\right)+\frac{6}{15}\coth^2\left(2\sqrt{x}+\frac{2\sqrt{t}}{15}\right). \tag{4.31}$$

The extended tanh method yielded novel and more general solutions, as shown above. So far as we're aware, these findings haven't been released. This solution can be used to explain the relativistic electron and the physical process of one-way stretching of weakly non-linear acoustic waves through a gas-filled pipe.

Graphical representations and physical discussion

Graphical representations of the solutions

In this section, for different values of the free parameter in the obtained solutions, we discuss portrayal illustration for expressed resolutions of the mentioned equations. These solutions give the highly stable

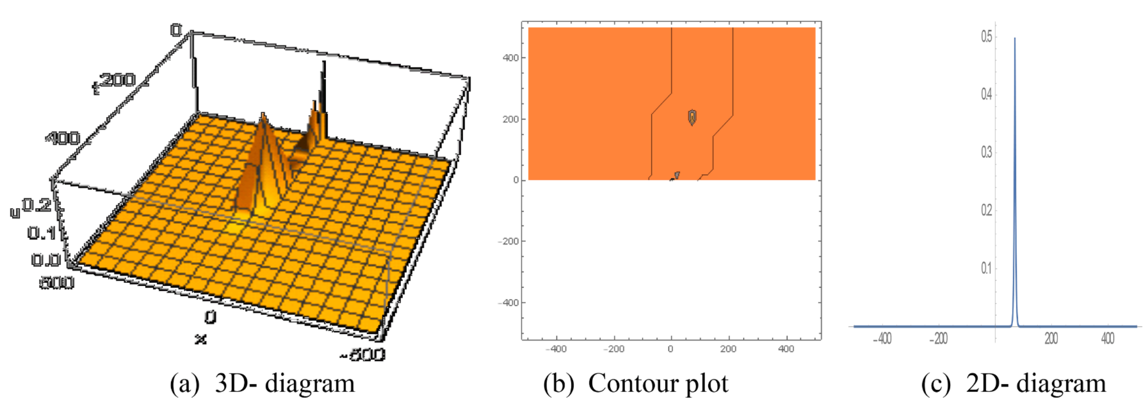

Fig. 4. The multiple singular soliton wave solution $u_4(x,t)$ within the intervals $-500 < x < 500$ and $0 < t < 500$.

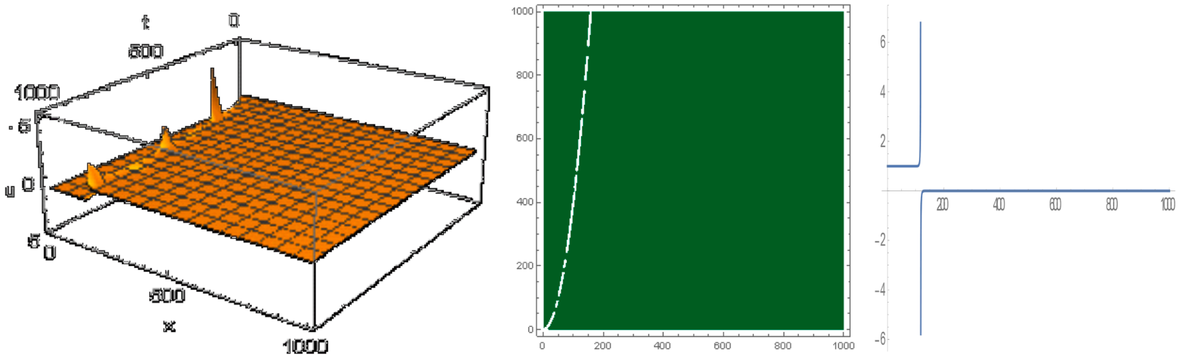

(a) 3D- diagram (b) Contour plot (c) 2D- diagram

Fig. 5. The multiple singular soliton wave solution $u_5(x,t)$ within the intervals $0 < x < 1000$ and $0 < t < 1000$.

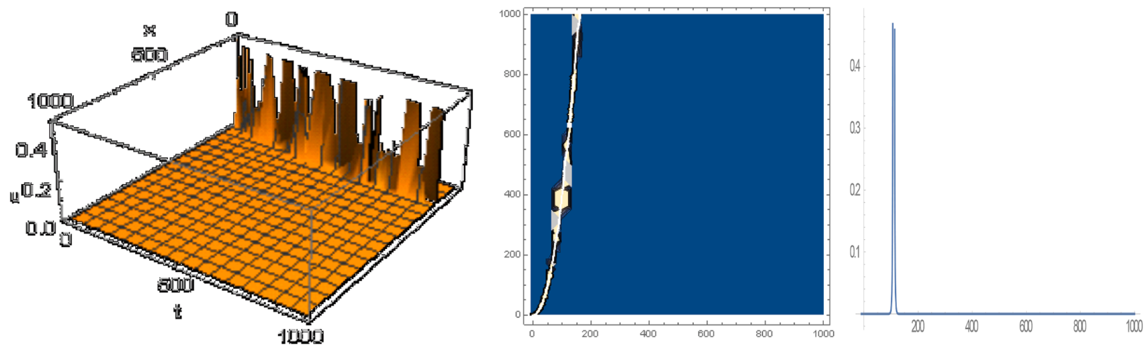

(a) 3D- diagram (b) Contour plot (c) 2D- diagram

Fig. 6. The multiple singular soliton wave solution $u_6(x,t)$ inside the intervals $-10 < x < 1000$ and $-10 < t < 1000$.

various types of solutions. They are depicted for the values $\mu = 1, \beta = 1$, $\alpha = \frac{1}{2}$ surrounded by different intermission for x and t. 3D, contour and 2D graphs of the solutions are investigated.

Physical interpretation of the solution

Herein sub-sector, the portrayal delegation in addition to description to the acquired resolutions of NLFDE over expressed equations are delimitating. Solutions $u_1(x,t), u_2(x,t), u_{15}(x,t)$ illustrate kink type solutions. Asymptotic waves that travel from one state to the next are known as kink waves. Fig. 1 and Fig. 2 which are represents TF-BF equation and Fig. 10 represents STF-RLW equation narrates the nature of the kink type resolution of $u_9(x,t), u_{10}(x,t), u_{11}(x,t), u_{12}(x,t)$ equation. The behavior of the shape of solution $u_1(x,t), u_2(x,t), u_{10}(x,t)$ is corresponding to the figure of solution $u_9(x,t), u_{10}(x,t), u_{11}(x,t)$, $u_{12}(x,t)$ hence for straightforwardness the quality of these accomplishment solutions are cropped here. The solutions of $u_3(x,t), u_{16}(x,t)$ represent the type of bell shape solution for the values $\mu = 1, \beta = 1, \alpha = \frac{1}{2}$ and $0 \le x \le 10, 0 \le t \le 10$ is denoted by Figs. 3 and 14which are represented TF-BF and STF-RLW equations, gradually. Fig. 4,5,6, and 13 earned this recitation are the multiple solitons solutions.

$u_4(x,t)$ for $\mu = 1, \beta = 1, \alpha = \frac{1}{2}$ and $-500 \le x \le 500$, $-500 \le t \le 500$, $u_5(x,t)$ for $\mu = 1, \beta = 1, \alpha = \frac{1}{2}$ and $0 \le x \le 1000$, $0 \le t \le 1000$, $u_6(x,t)$ for $\mu = 1, \beta = 1, \alpha = \frac{1}{2}$ and $-10 \le x \le 1000, -10 \le t \le 1000$ solutions of TF-BF equation and

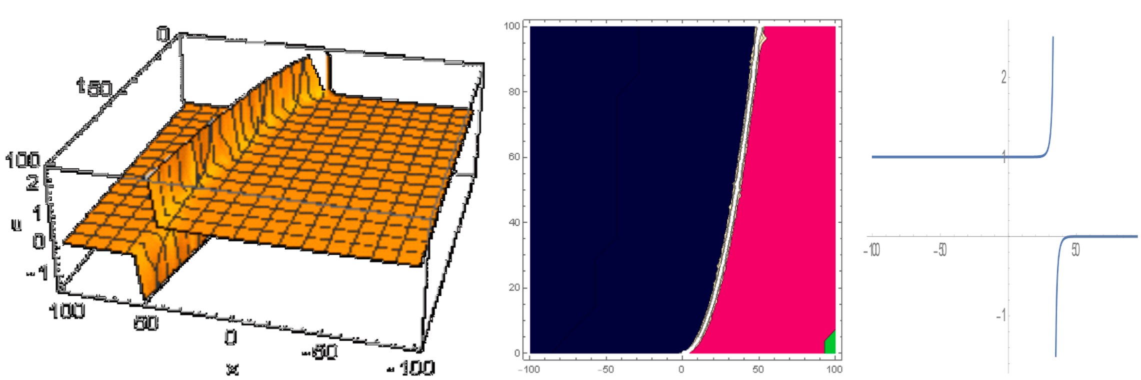

(a) 3D- diagram (b) Contour plot (c) 2D- diagram

Fig. 7. The periodic kink wave solution $u_7(x,t)$ within the intervals $-100 < x < 1000$ and $-10 < t < 100$.

$-10 < t < 100$

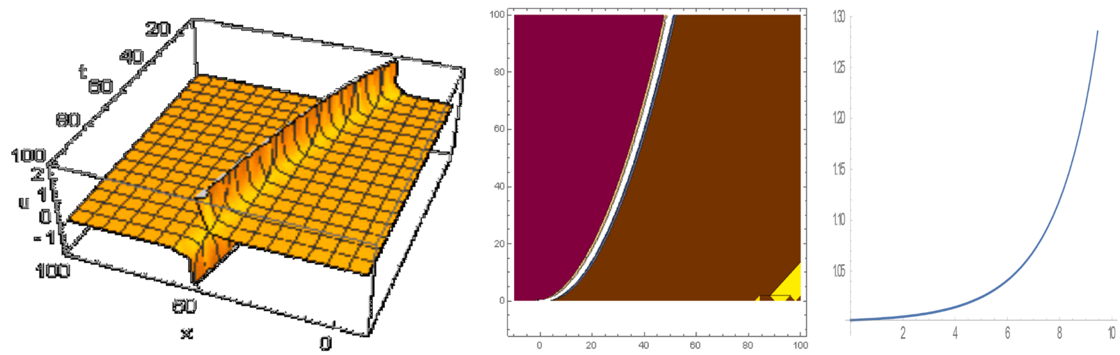

(a) 3D- diagram (b) Contour plot (c) 2D- diagram

Fig. 8. The singular kink wave solution $u_8(x,t)$ within the intervals $-10 < x < 100$ and $0 < t < 100$.

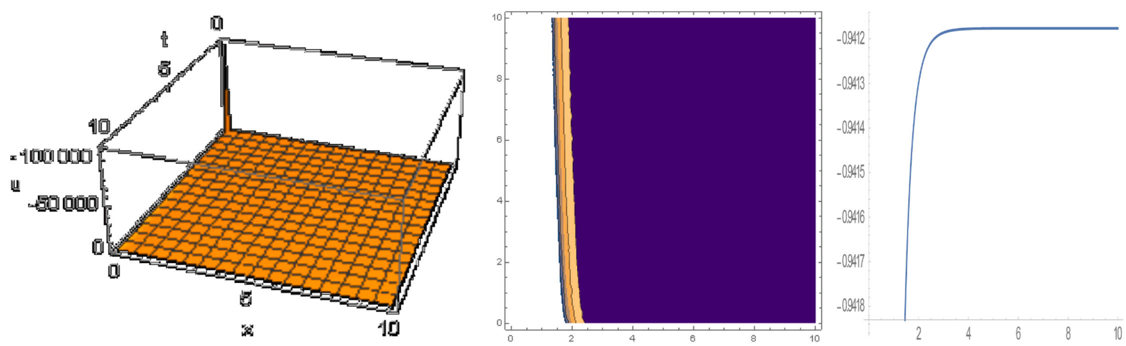

(a) 3D- diagram (b) Contour plot (c) 2D- diagram

Fig. 9. The singular kink wave solution $u_{13}(x,t)$ within the intervals $0 < x < 10$ and $0 < t < 10$.

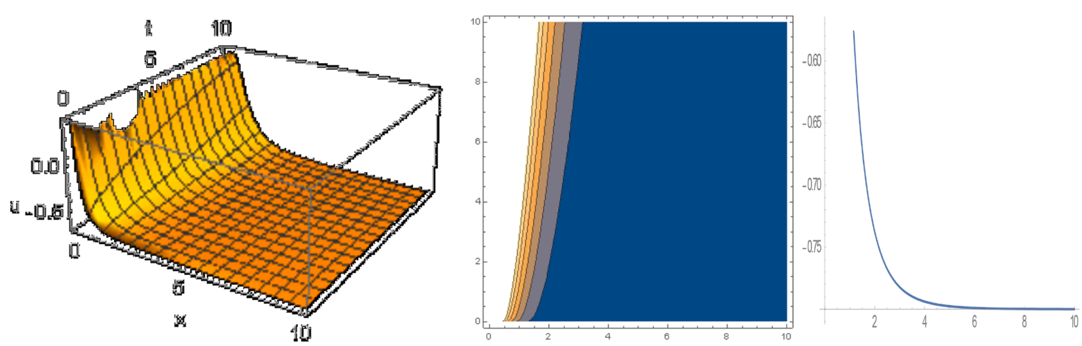

(a) 3D- diagram (b) Contour plot (c) 2D- diagram

Fig. 10. The kink wave solution $u_{15}(x,t)$ within the intervals $0 < x < 10$ and $0 < t < 10$.

$u_{23}(x,t)$ for $\mu = 1, \beta = 1, \alpha = \frac{1}{2}$ and $-10 \le x \le -100, -10 \le t \le -100$ narrates STF-RLW equation which all are multiple solitons solutions. $u_7(x,t)$ for $\mu = 1, \beta = 1, \alpha = \frac{1}{2}$ and $-10 \le x \le 1000, -10 \le t \le 1000$ obtained in this study for TF-BF equation is a periodic kink wave solution which is indicated in Fig. 7 and singular king wave solution in Fig. 8 is obtained from $u_8(x,t)$ for $\mu = 1, \beta = 1, \alpha = \frac{1}{2}$ and $-10 \le x \le 100$, $-10 \le t \le 100$. Also for TF-BF equation.$u_{13}(x,t)$, $u_{17}(x,t)$, for $\mu = 1, \beta = 1, \alpha = \frac{1}{2}$ and $0 \le x \le 10, 0 \le t \le$, for Figs. 9 and 11 (STF-RLW equation) gained in this study are the single soliton solution.$u_{13}(x,t)$ and $u_{17}(x,t)$ are resembling to the ardor of solution $u_{14}(x,t)$ for $\mu = 1, \beta = 1, \alpha = \frac{1}{2}$and $2 \le x \le 360$, $2 \le t \le 360 u_{20}(x,t)$, $u_{24}(x,t)$ for $\mu = 1, \beta = 1, \alpha = \frac{1}{2}$ and $10 \le x \le 100, 10 \le t \le 100$, $u_{22}(x,t)$ for $\mu = 1, \beta = 1, \alpha = \frac{1}{2}$ and $0 \le x \le 100, 0 \le t \le 100$ consequently for convenience these solutions are excluded here.

$u_{19}(x,t)$,$u_{21}(x,t)$ for $\mu = 1, \beta = 1, \alpha = \frac{1}{2}$ and $0 \le x \le -1000, 0 \le t \le -1000$ (STF-RLW equation) recites double solitons solutions shown in Fig. 12. $u_{18}(x,t)$ for $\mu = 1, \beta = 1, \alpha = \frac{1}{2}$ and $0 \le x \le .2, 0 \le t \le 2.5$ (STF- RLW equation) recites V-kink shape solution in Fig. 15.

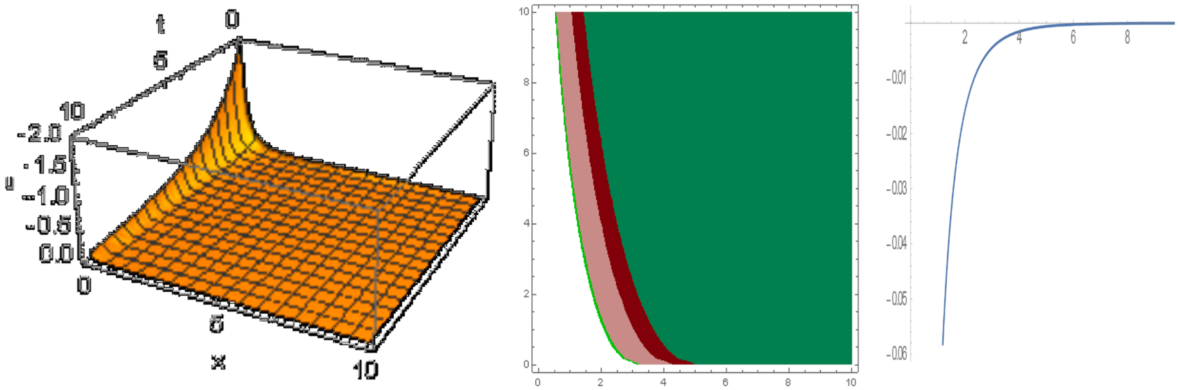

(a) 3D- diagram (b) Contour plot (c) 2D- diagram

Fig. 11. The singular soliton wave solution $u_{17}(x,t)$ within the intervals $0 < x < 10$ and $0 < t < 10$.

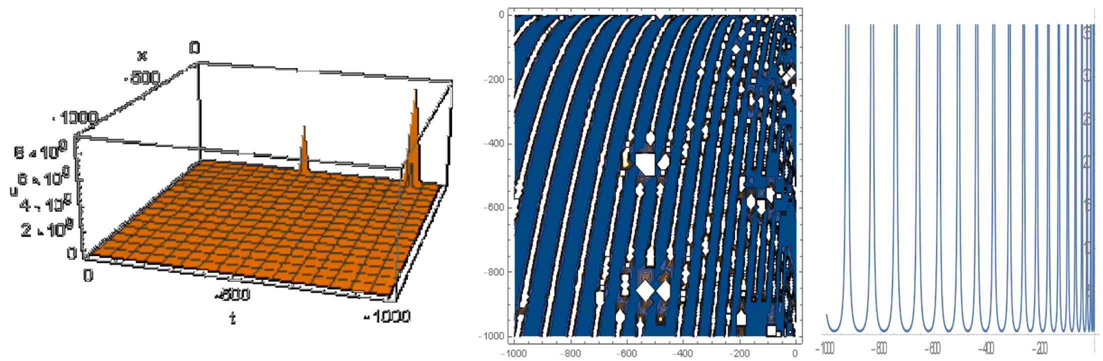

(a) 3D- diagram (b) Contour plot (c) 2D- diagram

Fig. 12. The double singular soliton wave solution $u_{19}(x,t)$ within the intervals $0 < x < -1000$ and $0 < t < -1000$.

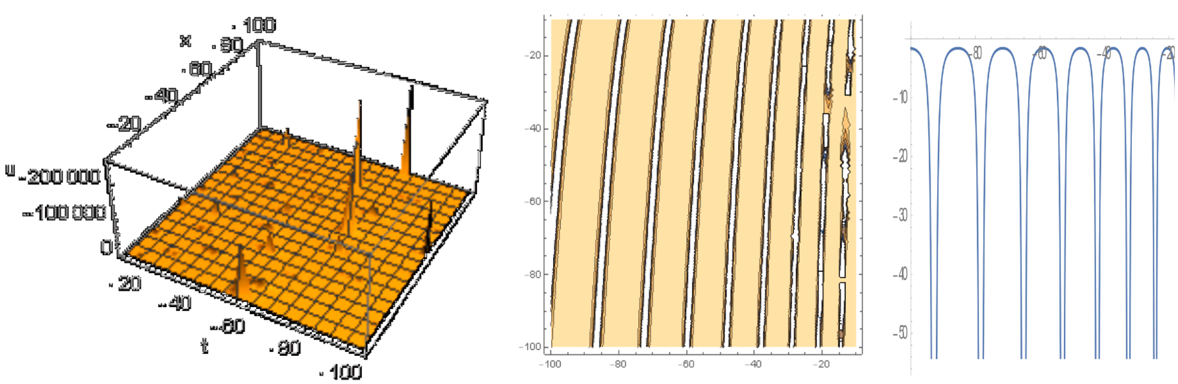

(a) 3D- diagram (b) Contour plot (c) 2D- diagram

Fig. 13. The multiple singular soliton wave solution $u_{23}(x,t)$ within the intervals $-10 < x < -100$ and $0 < t < -100$.

Conclusion

In this article, the ET-F method has been dispensed from finding several accurate answers. We have acquired abundant traveling wave solutions to the TF-BF equation along with the STF-RLW equation. It is constructed for these two equations, by the proposed method, different well-informed solitons, for the definite values of the free parameters like kink type, single soliton, double soliton, multiple solitons, and bell shape wave solutions. The results can be used to investigate gravitational water waves in long-wave occupancy, shallow water waves in coastal seas, hydro-magnetic waves in a cold plasma, phonetic waves in a cold plasma, hydrodynamics, and electromagnetic interactions, among many other things. To provide a more thorough study, 3D, 2D, and contour charts are used to better understand the two models' physical phenomena. Finally, the ET-F method gives a powerful mathematical tool for obtaining more precise traveling wave solutions to other nonlinear fractional evolution problems in several disciplines of applied sciences.

CRediT authorship contribution statement

M. Adel: Conceptualization, Funding acquisition, Methodology, Project administration, Software, Supervision, Visualization, Writing –

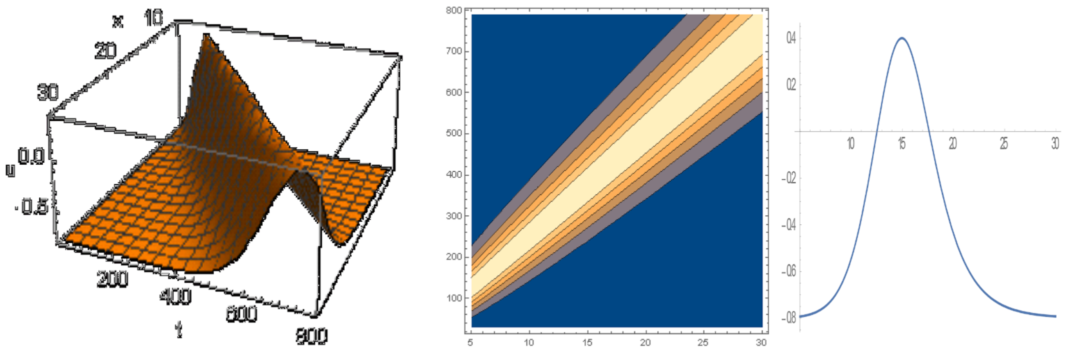

(a) 3D- diagram (b) Contour plot (c) 2D- diagram

Fig. 14. The bell type wave solution $u_{16}(x,t)$ within the intervals $5 < x < 30$ and $30 < t < 790$.

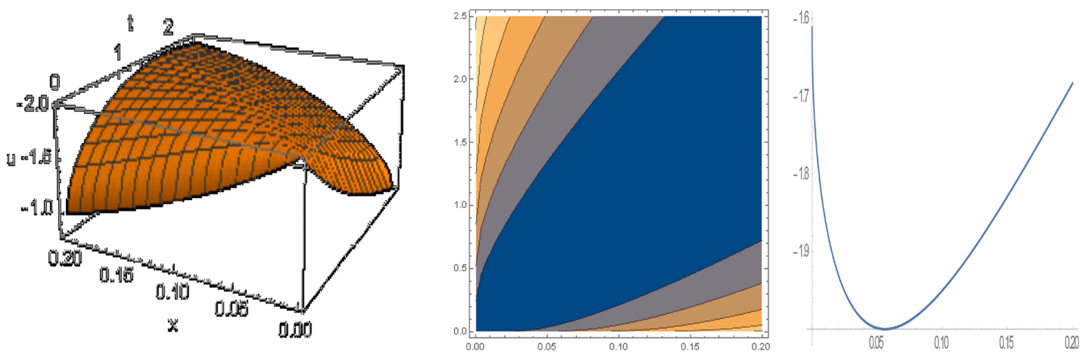

(a) 3D- diagram (b) Contour plot (c) 2D- diagram

Fig. 15. The V-kink type wave solution $u_{18}(x,t)$ within the intervals $0 < x < .2$ and $0 < t < 2.5$.

review & editing. **Dumitru Baleanu:** Conceptualization, Funding acquisition, Project administration, Supervision, Visualization, Writing – review & editing. **Umme Sadiya:** Data curation, Funding acquisition, Methodology, Software, Validation, Writing – review & editing. **Mohammad Asif Arefin:** Investigation, Data curation, Methodology, Validation, Software, Writing – review & editing. **M. Hafiz Uddin:** Data curation, Formal analysis, Investigation, Project administration, Resources, Validation, Visualization, Writing – original draft, Writing – review & editing. **Mahjoub A. Elamin:** Formal analysis, Investigation, Resources, Software, Visualization. **M.S. Osman:** Conceptualization, Data curation, Funding acquisition, Methodology, Resources, Supervision, Writing – original draft, Writing – review & editing.

Declaration of Competing Interest

The authors declare that they have no known competing financial interests or personal relationships that could have appeared to influence the work reported in this paper.

Acknowledgment

The researchers wish to extend their sincere gratitude to the Deanship of Scientific Research at the Islamic University of Madinah for the support provided to the Post-Publishing Program 1.

References

[1] Du M, Wang Z, Hu H. Measuring memory with the order of fractional derivative. Sci Rep 2013;3(1):1–3. https://doi.org/10.1038/srep03431.

[2] Shah K, Arfan M, Ullah A, Al-Mdallal Q, Ansari KJ, Abdeljawad T. Computational study on the dynamics of fractional order differential equations with applications. Chaos Soliton Fract 2022;157:111955. https://doi.org/10.1016/j.chaos.2022.111955.

[3] Shah K, Naz H, Sarwar M, Abdeljawad T. On spectral numerical method for variable-order partial differential equations. AIMS Math 2020;7(6):10422–38. https://doi.org/10.3934/math.2022581.

[4] Caputo M, Fabrizio M. A new definition of fractional derivative without singular kernel. Prog Fract Differ Appl 2015;1(2):73–85. https://doi.org/10.12785/pfda/010201.

[5] Zheng B. Exp-function method for solving fractional partial differential equations. Sci World J 2013;3:2013. https://doi.org/10.1155/2013/465723.

[6] Čermák J, Kisela T. Stability properties of two-term fractional differential equations. Nonlinear Dyn 2015;80(4):1673–84. https://doi.org/10.1007/s11071-014-1426-x.

[7] Ahmed E, Elgazzar AS. On fractional order differential equations model for nonlocal epidemics. Phys A Stat Mech Appl 2007;379(2):607–14. https://doi.org/10.1016/j.physa.2007.01.010.

[8] El-Sayed AMA, Behiry SH, Raslan WE. Adomian's decomposition method for solving an intermediate fractional advection-dispersion equation. Comput Math with Appl 2010;59(5):1759–65. https://doi.org/10.1016/j.camwa.2009.08.065.

[9] Ray SS. A new approach for the application of Adomian decomposition method for the solution of fractional space diffusion equation with insulated ends. Appl Math Comput 2008;202(2):544–9. https://doi.org/10.1016/j.amc.2008.02.043.

[10] El-Sayed AMA, Gaber M. The Adomian decomposition method for solving partial differential equations of fractal order in finite domains. Phys Lett Sect A Gen At Solid State Phys 2006;359(3):175–82. https://doi.org/10.1016/j.physleta.2006.06.024.

[11] Odibat Z, Momani S. A generalized differential transform method for linear partial differential equations of fractional order. Appl Math Lett 2008;21(2):194–9. https://doi.org/10.1016/j.aml.2007.02.022.

[12] Erturk VS, Momani S, Odibat Z. Application of generalized differential transform method to multi-order fractional differential equations. Commun Nonlinear Sci Numer Simul 2008;13(8):1642–54. https://doi.org/10.1016/j.cnsns.2007.02.006.

[13] Ji J, Zhang J, Dong Y. The fractional variational iteration method improved with the Adomian series. Appl Math Lett 2012;25(12):2223–6. https://doi.org/10.1016/j.aml.2012.06.007.

[14] Seadawy AR. Approximation solutions of derivative nonlinear Schrödinger equation with computational applications by variational method. Eur Phys J Plus 2015;130(9):1–10. https://doi.org/10.1140/epjp/i2015-15182-5.

[15] Guo S, Mei L. The fractional variational iteration method using He's polynomials. Phys Lett Sect A Gen At Solid State Phys 2011;375(3):309–13. https://doi.org/10.1016/j.physleta.2010.11.047.
[16] Song L, Zhang H. Solving the fractional BBM-Burgers equation using the homotopy analysis method. Chaos Solitons Fractals 2009;40(4):1616–22. https://doi.org/10.1016/j.chaos.2007.09.042.
[17] Arafa AAM, Rida SZ, Mohamed H. Homotopy analysis method for solving biological population model. Commun Theor Phys 2011;56(5):797–800. https://doi.org/10.1088/0253-6102/56/5/01.
[18] Inan B, Osman MS, Ak T, Baleanu D. Analytical and numerical solutions of mathematical biology models: The Newell-Whitehead-Segel and Allen-Cahn equations. Math method Appl Sci 2020;43(5):2588–600. https://doi.org/10.1002/mma.6067.
[19] Seadawy AR. The generalized nonlinear higher order of KdV equations from the higher order nonlinear Schrödinger equation and its solutions. Optik (Stuttg) 2017;139:31–43. https://doi.org/10.1016/j.ijleo.2017.03.086.
[20] Zheng B. (G′/G)-Expansion method for solving fractional partial differential equations in the theory of mathematical physics. Commun Theor Phys 2012;58(5):623–30. https://doi.org/10.1088/0253-6102/58/5/02.
[21] Ali KK, Wazwaz AM, Osman MS. Optical soliton solutions to the generalized nonautonomous nonlinear Schrödinger equations in optical fibers via the sine-Gordon expansion method. Optik 2020;208:164132. https://doi.org/10.1016/j.ijleo.2019.164132.
[22] Osman MS. Multiwave solutions of time-fractional (2+ 1)-dimensional Nizhnik–Novikov–Veselov equations. Pramana 2017;88(4):67. https://doi.org/10.1007/s12043-017-1374-3.
[23] Akbar MA, Ali NHM, Zayed EME. A generalized and improved (G′/G)-expansion method for nonlinear evolution equations. Math Probl Eng 2015;2012(September):2012. https://doi.org/10.1155/2012/459879.
[24] Qureshi S, Soomro A, Hincal E, Lee JR, Park C, Osman MS. An efficient variable stepsize rational method for stiff, singular and singularly perturbed problems. Alex Eng J 2022;61(12):10953–63. https://doi.org/10.1016/j.aej.2022.03.014.
[25] Arqub OA, Osman MS, Park C, Lee JR, Alsulami H, Alhodaly M. Development of the reproducing kernel Hilbert space algorithm for numerical pointwise solution of the time-fractional nonlocal reaction-diffusion equation. Alex Eng J 2022;61(12):10539–50. https://doi.org/10.1016/j.aej.2022.04.008.
[26] Tariq KU, Rezazadeh H, Zubair M, Osman MS, Akinyemi L. New Exact and Solitary Wave Solutions of Nonlinear Schamel–KdV Equation. Int J Appl Comput Math 2022;8(3).
[27] Ali Akbar M, Ali NHM. New solitary and periodic solutions of nonlinear evolution equation by exp-function method. World Appl Sci J 2012;17(12):1603–10.
[28] Lu B. Bäcklund transformation of fractional Riccati equation and its applications to nonlinear fractional partial differential equations. Phys Lett Sect A Gen At Solid State Phys 2012;376(28–29):2045–8. https://doi.org/10.1016/j.physleta.2012.05.013.
[29] Guo S, Mei L, Li Y, Sun Y. The improved fractional sub-equation method and its applications to the space-time fractional differential equations in fluid mechanics. Phys Lett Sect A Gen At Solid State Phys 2012;376(4):407–11. https://doi.org/10.1016/j.physleta.2011.10.056.
[30] Zhang S, Zhang HQ. Fractional sub-equation method and its applications to nonlinear fractional PDEs. Phys Lett Sect A Gen At Solid State Phys 2011;375(7):1069–73. https://doi.org/10.1016/j.physleta.2011.01.029.
[31] Lu B. The first integral method for some time fractional differential equations. J Math Anal Appl 2012;395(2):684–93. https://doi.org/10.1016/j.jmaa.2012.05.066.
[32] Arqub OA, Osman MS, Abdel-Aty AH, Mohamed ABA, Momani S. A numerical algorithm for the solutions of ABC singular Lane-Emden type models arising in astrophysics using reproducing kernel discretization method. Mathematics 2020;8(6):923. https://doi.org/10.3390/math8060923.
[33] Hafiz Uddin M. Close Form Solutions of the Fractional Generalized Reaction Duffing Model and the Density Dependent Fractional Diffusion Reaction Equation. Appl Comput Math 2017;6(4):177. https://doi.org/10.11648/j.acm.20170604.13.
[34] Li LX, Li EQ, Wang ML. The (G′/G, 1/G)-expansion method and its application to travelling wave solutions of the Zakharov equations. Appl Math 2010;25(4):454–62. https://doi.org/10.1007/s11766-010-2128-x.
[35] Zayed EME, Abdelaziz MAM. The two-variable (G′/G,1/G)-expansion method for solving the nonlinear KdV-mKdV equation. Math Probl Eng 2012;2012. https://doi.org/10.1155/2012/725061.
[36] Ali S, Khan A, Shah K, Alqudah MA, Abdeljawad T, Siraj-ul-Islam. On computational analysis of highly nonlinear model addressing real world applications. Result Phys 2022;36. https://doi.org/10.1016/j.rinp.2022.105431.
[37] Azam M, Xu T, Khan M. Numerical simulation for variable thermal properties and heat source/sink in flow of Cross nanofluid over a moving cylinder. Int Commun Heat Mass Trans 2020;118:104832. https://doi.org/10.1016/j.icheatmasstransfer.2020.104832.
[38] Ghanbari B, Osman MS, Baleanu D. Generalized exponential rational function method for extended Zakharov-Kuzetsov equation with conformable derivative. Mod Phys Lett A 2019;34(20):1950155. https://doi.org/10.1142/S0217732319501554.
[39] Osman MS, Ghanbari B. New optical solitary wave solutions of Fokas-Lenells equation in presence of perturbation terms by a novel approach. Optik 2018;175:328–33. https://doi.org/10.1016/j.ijleo.2018.08.007.
[40] Azam M, Xu T, Shakoor A, Khan M. Effects of Arrhenius activation energy in development of covalent bonding in axisymmetric flow of radiative-Cross nanofluid. Int Commun Heat Mass Trans 2020;113:104547. https://doi.org/10.1016/j.icheatmasstransfer.2020.104547.
[41] Azam M, Mabood F, Xu T, Waly M, Tlili I. Entropy optimized radiative heat transportation in axisymmetric flow of Williamson nanofluid with activation energy. Result Phys 2020;19:103576. https://doi.org/10.1016/j.rinp.2020.103576.
[42] Azam M, Xu T, Mabood F, Khan M. Non-linear radiative bioconvection flow of cross nano-material with gyrotatic microorganisms and activation energy. Int Commun Heat Mass Trans 2021;127:105530. https://doi.org/10.1016/j.icheatmasstransfer.2021.105530.
[43] Osman MS. One-soliton shaping and inelastic collision between double solitons in the fifth-order variable-coefficient Sawada-Kotera equation. Nonlinear Dyn 2019;96(2):1491–6. https://doi.org/10.1007/s11071-019-04866-1.
[44] Rezazadeh H, Osman MS, Eslami M, Ekici M, Sonmezoglu A, Asma M, et al. Mitigating Internet bottleneck with fractional temporal evolution of optical solitons having quadratic–cubic nonlinearity. Optik 2018;164:84–92.
[45] Hashemi MS, Baleanu D. On the Time Fractional Generalized Fisher Equation: Group Similarities and Analytical Solutions. Commun Theor Phys 2016;65(1):11–6. https://doi.org/10.1088/0253-6102/65/1/11.
[46] Burgers JM. A Mathematical Model Illustrating the Theory of Turbulence. no. C Adv Appl Mech 1948;1:171–99. https://doi.org/10.1016/S0065-2156(08)70100-5.
[47] Lax PD. "Hyperbolic Systems of Conservation Laws and the Mathematical Theory of Shock Waves", *Hyperbolic Syst*. Conserv Laws Math Theory Shock Waves 1973. https://doi.org/10.1137/1.9781611970562.
[48] Jiang Y, Wei T, Zhou X. Stochastic generalized Burgers equations driven by fractional noises. J Differ Equ 2012;252(2):1934–61. https://doi.org/10.1016/j.jde.2011.07.032.
[49] Garra R. Fractional-calculus model for temperature and pressure waves in fluid-saturated porous rocks. Phys Rev E - Stat Nonlinear, Soft Matter Phys 2011;84(3):1–6. https://doi.org/10.1103/PhysRevE.84.036605.
[50] Inc M. The approximate and exact solutions of the space- and time-fractional Burgers equations with initial conditions by variational iteration method. J Math Anal Appl 2008;345(1):476–84. https://doi.org/10.1016/j.jmaa.2008.04.007.
[51] Inc M. On numerical solution of Burgers' equation by homotopy analysis method. Phys Lett Sect A Gen At Solid State Phys 2008;372(4):356–60. https://doi.org/10.1016/j.physleta.2007.07.057.
[52] Ross J, Villaverde AF, Banga JR, Vázquez S, Morán F. A generalized Fisher equation and its utility in chemical kinetics. Proc Natl Acad Sci U S A 2010;107(29):12777–81. https://doi.org/10.1073/pnas.1008257107.
[53] Wazwaz AM. The tanh method for generalized forms of nonlinear heat conduction and Burgers-Fisher equations. Appl Math Comput 2005;169(1):321–38. https://doi.org/10.1016/j.amc.2004.09.054.
[54] Merdan M. Solutions of time-fractional reaction-diffusion equation with modified Riemann-Liouville derivative. Int J Phys Sci 2012;7(15):2317–26. https://doi.org/10.5897/ijps12.027.
[55] Kenkre VM. Results from variants of the Fisher equation in the study of epidemics and bacteria. Phys A Stat Mech its Appl 2004;vol. 342, no. 1–2 SPEC. ISS:242–8. https://doi.org/10.1016/j.physa.2004.04.084.
[56] Yokus A, Yavuz M. Novel comparison of numerical and analytical methods for fractional Burger-Fisher equation. Discrete Contin Dyn Syst -S 2021;14(7):2591–606. https://doi.org/10.3934/dcdss.2020258.
[57] Peregrine DH. Calculations of the development of an undular bore. J Fluid Mech 1966;25(2):321–30. https://doi.org/10.1017/S0022112066001678.
[58] Fu CL. Simplified Tikhonov and Fourier regularization methods on a general sideways parabolic equation. J Comput Appl Math 2004;167(2):449–63. https://doi.org/10.1016/j.cam.2003.10.011.
[59] Yang F, Fu CL. The method of simplified Tikhonov regularization for dealing with the inverse time-dependent heat source problem. Comput Math Appl 2010;60(5):1228–36. https://doi.org/10.1016/j.camwa.2010.06.004.
[60] Yang F, Fu CL. A simplified Tikhonov regularization method for determining the heat source. Appl Math Model 2010;34(11):3286–99. https://doi.org/10.1016/j.apm.2010.02.020.
[61] Hohage T. Regularization of exponentially ill-posed problems. Numer Funct Anal Optim 2000;21(3):439–64. https://doi.org/10.1080/01630560008816965.
[62] Mohammadi M, Mokhtari R. Solving the generalized regularized long wave equation on the basis of a reproducing kernel space. J Comput Appl Math 2011;235(14):4003–14. https://doi.org/10.1016/j.cam.2011.02.012.
[63] Khalil EM, Korpinar Z, Inc M. Investigation of numerical solutions of fractional generalized regularized long wave equations by least squares-residual power series method. Phys Scr 2021;96(9):094005. https://doi.org/10.1088/1402-4896/ac0865.
[64] Khalil R, Al Horani M, Yousef A, Sababheh M. A new definition of fractional derivative. J Comput Appl Math 2014;264:65–70. https://doi.org/10.1016/j.cam.2014.01.002.
[65] Wazwaz AM. The extended tanh method for abundant solitary wave solutions of nonlinear wave equations. Appl Math Comput 2007;187(2):1131–42. https://doi.org/10.1016/j.amc.2006.09.013.